

Large tunneling anisotropic magnetoresistance in (Ga,Mn)As nanoconstrictions

A.D. Giddings,^{1,2} M.N. Khalid,² J. Wunderlich,² S. Yasin,³ R.P. Campion,¹ K.W. Edmonds,¹ J. Sinova,⁴ T. Jungwirth,^{5,1} K. Ito,² K. Y. Wang,¹ D. Williams,² B.L. Gallagher,¹ and C.T. Foxon¹

¹*School of Physics and Astronomy, University of Nottingham, Nottingham NG7 2RD, UK*

²*Hitachi Cambridge Laboratory, Cambridge CB3 0HE, UK*

³*University of Cambridge, UK*

⁴*Department of Physics, Texas A&M University, College Station, TX 77843-4242, USA*

⁵*Institute of Physics ASCR, Cukrovarnick 10, 162 53 Praha 6, Czech Republic*

(Dated: September 23, 2018)

We report a large tunneling anisotropic magnetoresistance (TAMR) in a thin (Ga,Mn)As epilayer with lateral nanoconstrictions. The observation establishes the generic nature of this effect, which originates from the spin-orbit coupling in a ferromagnet and is not specific to a particular tunnel device design. The lateral geometry allows us to link directly normal anisotropic magnetoresistance (AMR) and TAMR. This indicates that TAMR may be observable in other materials showing a comparable AMR at room temperature, such as transition metal alloys.

PACS numbers: 75.50.Pp, 85.75.Mm

The family of (III,Mn)V ferromagnetic semiconductors offers unique opportunities for exploring the integration of two frontier areas in information technologies: spintronics and nanoelectronics. A striking example of the synergy of the two fields is the very large magnetoresistance (MR) effect recently observed in lithographically defined (Ga,Mn)As nanostructures in which tunnel barriers are formed in sub-10 nm lateral constrictions [1]. The structure studied in Ref. [1] consists of two such constrictions dividing a lithographically defined (Ga,Mn)As wire into contact leads and a narrower central region. The observed $\sim 2000\%$ spin-valve like signal was interpreted as a type of tunneling MR (TMR) effect arising from the relative alignment of the magnetizations in the regions on either side of the constriction, and in which the barrier shape was spin dependent. This experiment is clearly of great importance as the size of the effect indicates that nanospintronic structures may provide a new route to memory and sensor devices.

Recently, seemingly unrelated strongly anisotropic hysteretic MR of magnitude $\sim 3\%$ was reported [2] in a (Ga,Mn)As/AlOx/Au tunneling device. The effect is not due to the normal TMR as only a single ferromagnetic layer is present. It is a manifestation of a novel tunneling anisotropic MR (TAMR) effect that had been previously overlooked. The TAMR arises directly from the spin-orbit (SO) coupling induced dependence of the tunneling density of states of the ferromagnetic layer on the orientation of the magnetization with respect to the crystallographic axes [2].

In this paper we report that TAMR effects can also dominate the MR response of (Ga,Mn)As nanoconstrictions. It establishes that TAMR is a generic phenomenon whose occurrence is not dependent upon a particular device structure. The TAMR signals we observe are of order 100%. We note that very recent low-temperature studies of (Ga,Mn)As/GaAs/(Ga,Mn)As vertical tunnel struc-

tures find that the TAMR can be much larger than typical TMR signals in metallic magnetic tunnel junctions and astonishingly can even lead to the realization of a full MR current switch [3]. Our lateral microstructures make it possible to study the link between the normal anisotropic MR (AMR) [4, 5] in devices without constrictions, which also originates from the SO coupled band structure and is present in many metallic ferromagnets [6], and TAMR measured across a tunnel junction.

The lateral geometry of the devices is shown in Fig. 1(a). All microstructures discussed in this paper were fabricated on a single $\text{Ga}_{0.98}\text{Mn}_{0.02}\text{As}$ epilayer grown along the [001] crystal axis by low-temperature molecular beam epitaxy [7]. Despite being only 5 nm thick the layer has a Curie temperature of 40 K and conductivity of $130 \Omega^{-1} \text{cm}^{-1}$ at room temperature: values which are comparable with those achieved in high quality thicker layers for 2% Mn. Device fabrication was carried out by e-beam lithography using PMMA positive resist and reactive ion etching.

The $3 \mu\text{m}$ wide Hall bar, aligned along the [110] direction, has pairs of constrictions from 30 nm to 400 nm wide separated by a distance of $9 \mu\text{m}$. For reference AMR experiments, a separate unstructured bar was fabricated in parallel to the stripe without constrictions. Four point I-V curves and resistances were measured for both the unstructured Hall bars and across the constrictions (see Fig.1(a)). A standard low frequency lock-in technique was used.

The comparison of MR characteristics of different devices is presented in Fig. 1(b) for external magnetic field applied parallel to the stripe (parallel to current). The unstructured bar and the 100 nm constriction show MRs typical of the bulk (Ga,Mn)As epilayers [4, 8]. The overall isotropic (independent of applied field orientation) negative MR in these traces is attributed to the suppression of magnetic disorder at large fields [4]. The hys-

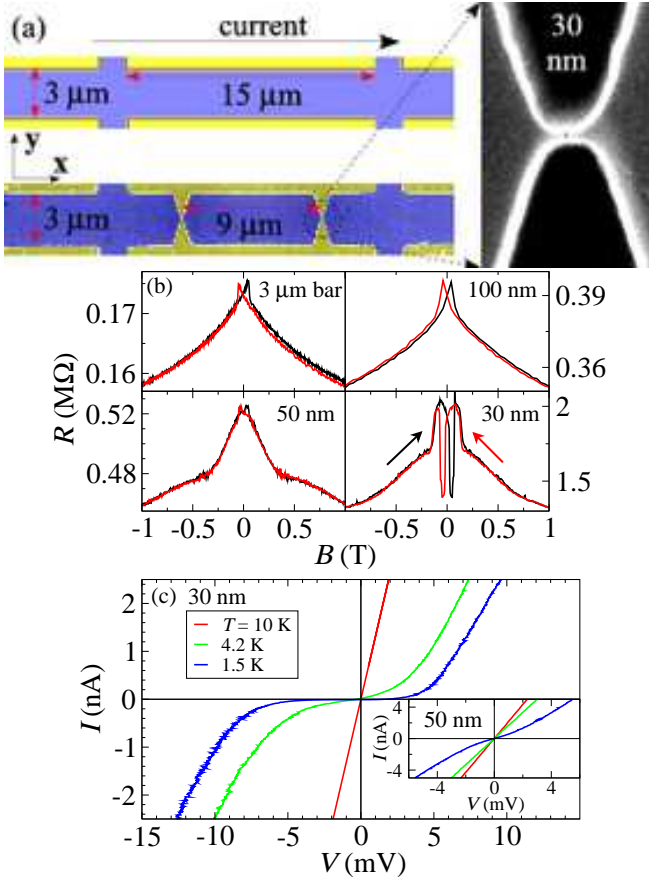


FIG. 1: (a) Schematic of an unstructured bar and SEM image of a double constricted nanodevice. (b) Magnetotransport measurements for unstricted and constricted devices with applied field parallel to current at a temperature of 4.2 K (c) I-V characteristics for the 30 nm constriction device and the 50 nm device (inset)

teretic low field effect is associated with the magnetization reversal and since its magnitude and sense change with applied field orientation it is a manifestation of the AMR. The shape of the 50 nm constriction MR partly deviates from this normal bulk (Ga,Mn)As behavior and a dramatic change is observed in the 30 nm constriction, both in the size and the sign of the low-field effect. The marked increase of the overall resistance of the 30 nm constriction device suggests that the anomalies occur due to the formation of a tunnel junction. This is confirmed by the measured temperature dependence of the I-V curves. Constrictions greater than 100 nm have Ohmic behavior. As shown in Fig. 1(c), deviations become more pronounced as the constriction size and temperature is reduced. At low temperature and bias, conduction through the 30 nm constrictions is by tunneling. The occurrence of tunneling in such a wide constriction suggests that disorder in the very thin, low Mn density (Ga,Mn)As material leads to local depletion and a tunnel barrier of lateral width considerably smaller than the

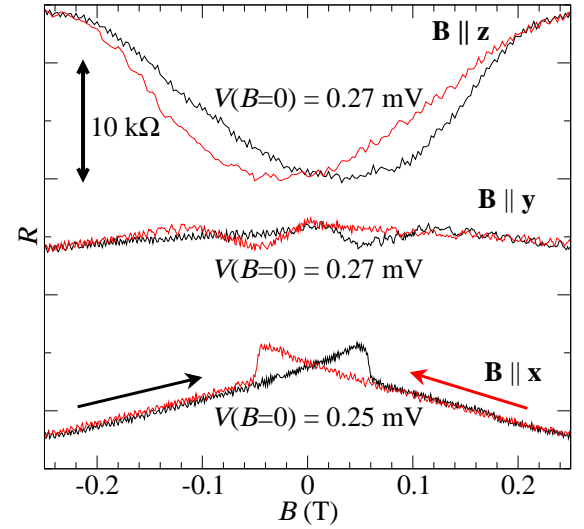


FIG. 2: Low field magnetotransport measurements for the unstructured bar with applied field in three orthogonal orientations at a temperature of 4.2 K.

nominal physical width.

The negative sign of the hysteretic effect in our tunneling device is incompatible with TMR, for which antiparallel alignment on either side of the constriction at intermediate fields would lead to a positive hysteretic effect in the present geometry. Instead, we interpret the data as the TAMR which can show both the normal and inverted spin-valve like signals depending on the applied field orientation [2, 3]. This interpretation is also consistent with the geometry of our lateral device in which the central region between constrictions and leads have the same, relatively large, width and are therefore expected to reverse simultaneously.

We now present a detailed analysis of the anisotropic magnetotransport characteristics of our devices. In Fig. 2 we plot the low-field AMR characteristics of the unstructured bar for magnetic fields applied parallel to the stripe ($B \parallel x$), perpendicular to the stripe in-plane ($B \parallel y$), and perpendicular to the stripe out-of-plane ($B \parallel z$). The three curves in the figure are offset for clarity and also because the absolute comparison between resistances for different field orientations is impossible due to our experimental set up which does not allow us to rotate the sample in the cryostat during the measurement. Each thermal cycling of the sample leads to overall resistance shifts comparable to the size of the anisotropic magnetotransport effects. Apart from this constant offset the MR traces are reproducible which allows us to analyze the magnetotransport anisotropies based on the low-field parts of individual MRs.

We associate the hysteretic steps in the two lower curves in Fig. 2 with in-plane magnetization reversal precesses. A much stronger MR response is observed in the upper curve with the resistance increas-

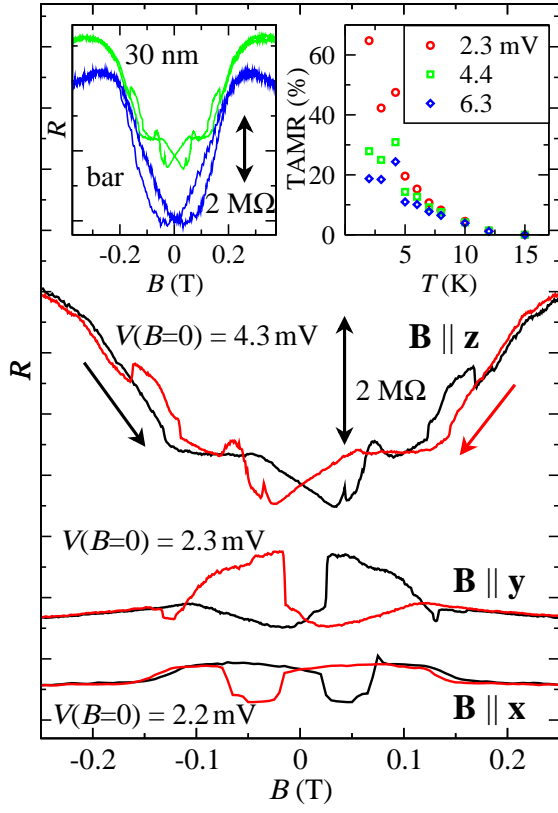


FIG. 3: Detail of the TMR measured in the 30 nm constrictions with applied field in the three orthogonal directions. Left inset: comparison of the perpendicular to plane AMR of the unstricted stripe with the TMR of the 30 nm constriction. The graph for the bar has been scaled up 300 times. Right inset: the temperature dependence of the TMR for three different voltages, with $B \parallel x$.

ing as the magnetization is rotated from the epilayer plane towards the vertical z -direction. In previously studied 50 nm thin $\text{Ga}_{0.98}\text{Mn}_{0.02}\text{As}$ epilayers there was virtually no difference in the magnitude of the AMR for the two perpendicular-to-current orientations. The large (8%) out-of-plane AMR we observe is therefore attributed to the strong vertical confinement of the carriers in our ultra-thin $\text{Ga}_{0.98}\text{Mn}_{0.02}\text{As}$ epilayer which breaks the symmetry between states with magnetization $\mathbf{M} \parallel \mathbf{y}$ and $\mathbf{M} \parallel \mathbf{z}$. Another indication of confinement effects is the presence of hysteresis in the $B \parallel z$ MR. In thicker $\text{Ga}_{0.98}\text{Mn}_{0.02}\text{As}$ epilayers the growth direction is magnetically hard with zero remanence due to a small compressive strain induced by the GaAs substrate and due to the shape anisotropy [8, 9]. These effects compete in our epilayer with an increase in the relative population of the heavy hole states due to the confinement, which tends to favor spin polarization along the growth direction [10] and therefore changes the magnetic anisotropy energy landscape.

The dominance of the TMR effect in the tunneling

regime is clearly demonstrated in Fig. 3. This shows that the measured MR is quite different for the three orthogonal applied field directions. The comparable magnitude but opposite sign of the TMR for $B \parallel x$ and $B \parallel y$, indicates that the low resistance tunneling state is for $\mathbf{M} \parallel \mathbf{y}$ and the high resistance state for $\mathbf{M} \parallel \mathbf{x}$, and that the in-plane reversal process involves 90° switching through the two axes. In the right inset of Fig. 3 we plot temperature dependence of the TMR for several excitation voltages. For the lowest temperature in the figure, $T = 2 \text{ K}$, and lowest voltage, $V = 2.3 \text{ mV}$, we obtain a 65% in-plane TMR and the curves show no signs of saturation at these values. Even larger TMR signals are recorded when \mathbf{M} is rotated out of the (Ga,Mn)As epilayer plane. For $V = 4.3 \text{ mV}$ and $T = 4.2 \text{ K}$ we obtained a 110% TMR for $\mathbf{M} \parallel \mathbf{z}$ which compares to only 31% for $\mathbf{M} \parallel \mathbf{x}$ at the same temperature and excitation voltage.

The close correspondence between the AMR results of Fig. 2 and the TMR results of Fig. 3 is evident. The switching events in the in-plane MR traces occur at comparable magnetic fields for the two devices. In both the AMR and the TMR experiments, the effects at $B \parallel x$ and $B \parallel y$ have a similar magnitude and the opposite sign. (Note that the high and low resistance states switch places in the AMR and TMR traces which is not surprising given the different transport regimes of the two devices.) The most important comparison is between the $B \parallel z$ AMR and TMR as we expect the hysteretic magnetization to be unaffected by the constriction as it approaches saturation. The inset of Fig. 3 shows the expected similarity in general form and field scale of the AMR and TMR in this geometry. The observation that the magnitude of the TMR is considerably larger for $B \parallel z$ than for the in-plane fields as is the case for the AMR, is another manifestation of the direct link between the AMR and TMR effects. The fact that the observed TMR effects are all much larger than the AMR effects is a manifestation of the general high sensitivity of tunneling probabilities compared to ohmic transport coefficients.

The AMR in (Ga,Mn)As was successfully modeled [5] within the Boltzmann transport theory that accounts for the SO induced anisotropies with respect to the magnetization orientation in the hole group velocities and scattering rates. The TMR has been analyzed in terms of tunneling density of states anisotropies [2, 3] or by calculating the transmission coefficient anisotropies using the Landauer formalism [11, 12]. Both approaches confirmed the presence of the TMR effects. The density of states calculations also provided additional qualitative interpretation of the measured field-angle and temperature dependence of TMR in the vertical tunnel structures [2, 3]. The (Ga,Mn)As band structure in these calculations is obtained using the $\mathbf{k} \cdot \mathbf{p}$ envelope function description of the host semiconductor valence bands in the presence of an effective kinetic-exchange field pro-

duced by the polarized local Mn moments [9].

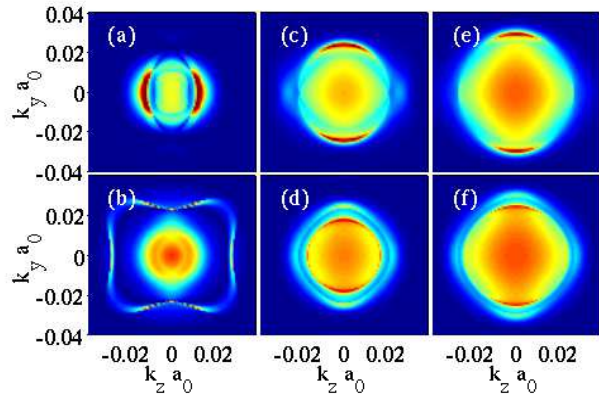


FIG. 4: Color plot of the calculated tunneling transmission probabilities vs. conserved in-plane momenta at the Fermi energy. The carrier densities are 0.01 nm^{-3} (a,b), 0.05 nm^{-3} (c,d), and 0.1 nm^{-3} (e,f). The barrier height and width are 1 eV and 2 nm, respectively. Red is the highest probability for a given density and blue is zero. The tunneling current is along the x -direction and the magnetization is oriented along the z -direction for the first row and along the x -direction for the second row.

In Fig. 4 we plot illustrative Landauer transmission probabilities at the Fermi energy as a function of conserved momenta in the (k_z, k_y) -plane for two semi-infinite 3D (Ga,Mn)As regions separated by a tunnel barrier. The tunnel current is along the x -direction. In both ferromagnetic semiconductor contacts we consider substitutional Mn doping of 2% and a growth direction strain of 0.2%. Details of such calculations can be found in Ref. 12. The additional component of the strain, which was not considered in previous Landauer transport studies, allows us to model the broken cubic symmetry effects observed in experimental TAMR [2, 3]. The bulk 3D hole densities in our (Ga,Mn)As epilayer are of order $1 \times 10^{20} \text{ cm}^{-3}$ and a gradual depletion of the carriers is expected near the tunnel constriction. Data in panels (a) and (b) correspond to hole density $0.1 \times 10^{20} \text{ cm}^{-3}$, in (c) and (d) to density $0.5 \times 10^{20} \text{ cm}^{-3}$, and in (e) and (f) to $1 \times 10^{20} \text{ cm}^{-3}$.

The diagrams in Fig. 4 show an intricate dependence of the theoretical TAMR on the position in the (k_z, k_y) -plane. When integrated over all states at the Fermi energy, the TAMR ranges between $\sim 50\%$ and $\sim 1\%$ for the studied hole densities $0.1\text{--}1 \times 10^{20} \text{ cm}^{-3}$. In the experimental structure, however, the (Ga,Mn)As is strongly confined in the growth direction which leads to depopulation of high k_z momenta states. The tunnel constriction further reduces the number of k_y -states contributing to the signal. Classically, the current is carried only by particles with small momenta in the x and y -directions and wave-mechanics adds a condition $k_y = \pm\pi/w$, where w is the effective width of the constriction. Fig. 4 illustrates that the theoretical TAMR can change significantly de-

pending on the k_z and k_y values selected by the confinements which suggests that both the magnitude and sign of the effect are strongly sensitive to the detailed parameters of the tunnel barrier and of the ferromagnetic semiconductor epilayer.

To conclude, we have established the TAMR as a generic effect in tunnel devices with SO coupled ferromagnetic contacts. The anisotropic transport nature of the large MR signal in our lateral device was demonstrated by directly comparing the TAMR with the AMR effects in the contact leads. Our measurements open a new avenue for integration of spintronics through the TAMR with semiconductor nanoelectronics and motivate studies of the effect in other materials showing the AMR, including high Curie temperature ferromagnetic metals.

The authors thank L. Eaves, C. Gould, A.H. MacDonald, L. Molenkamp, and P. Novák for useful discussions and acknowledge financial support from the Grant Agency of the Czech Republic through grant 202/02/0912, from the EU FENIKS project EC:G5RD-CT-2001-00535, and from the UK EPSRC through grant GR/S81407/01.

-
- [1] C. Ruester, T. Borzenko, C. Gould, G. Schmidt, L. Molenkamp, X. Liu, T. Wojtowicz, J. Furdyna, Z. Yu, and M. Flatté, *Phys. Rev. Lett.* **91**, 216602 (2003).
 - [2] C. Gould, C. Rüster, T. Jungwirth, E. Girgis, G. M. Schott, R. Giraud, K. Brunner, G. Schmidt, and L. Molenkamp (2004), *cond-mat/0407735*.
 - [3] C. Ruester, C. Gould, T. Jungwirth, J. Sinova, G. Schott, R. Giraud, K. Brunner, G. Schmidt, and L. Molenkamp (2004), *cond-mat/0408532*.
 - [4] D. V. Baxter, D. Ruzmetov, J. Scherschligt, Y. Sasaki, X. Liu, J. K. Furdyna, and C. H. Mielke, *Phys. Rev. B* **65**, 212407 (2002).
 - [5] T. Jungwirth, J. Sinova, K. Wang, K. W. Edmonds, R. Campion, B. Gallagher, C. Foxon, Q. Niu, and A. MacDonald, *Appl. Phys. Lett.* **83**, 320 (2003).
 - [6] O. Jaoul, I. A. Campbell, and A. Fert, *J. Magn. Mater.* **5**, 23 (1977).
 - [7] R. Campion, K. Edmonds, L. Zhao, K. Wang, C. Foxon, B. Gallagher, and C. Staddon, *J. Cryst. Growth* **247**, 42 (2003).
 - [8] K. Wang, K. Edmonds, R. Campion, L. Zhao, A. Neumann, C. Foxon, B. Gallagher, and P. Main, in *Proceedings of the ICPS-26* (IOP publishing, UK, 2002), p. 58.
 - [9] J. König, J. Schliemann, T. Jungwirth, and A. MacDonald, in *Electronic Structure and Magnetism of Complex Materials*, edited by D. Singh and D. Papaconstantopoulos (Springer Verlag, Berlin, 2003).
 - [10] B. Lee, T. Jungwirth, and A. MacDonald, *Semicond. Sci. Technol.* **17**, 393 (2002).
 - [11] L. Brey, C. Tejedor, and J. Fernández-Rossier (2004), *cond-mat/0405473*.
 - [12] A. G. Petukhov, A. N. Chantis, and D. O. Demchenko, *Phys. Rev. Lett.* **89**, 107205 (2002).